

A WATER SPECTROSCOPY MICROSYSTEM WITH INTEGRATED DISCHARGE SOURCE, DISPERSION OPTICS, AND SAMPLE DELIVERY

Long Que, Chester G. Wilson, J.-A. Esclafer de La Rode and Yogesh B. Gianchandani
*Department of Electrical Engineering and Computer Science
 University of Michigan, Ann Arbor*

ABSTRACT

This paper reports a microsystem integrating the fluidic, electrical and optical elements required for field-portable water-chemistry testing by electric discharge spectroscopy. The device utilizes a DC microdischarge as a spectroscopic source. The discharge is created by applying a DC voltage between a metal anode and uses the water sample as the cathode. Impurities are sputtered from the water sample into the microdischarge. A blazed grating is used as the dispersion element, along with an aperture fabricated on a glass substrate. The microsystem is assembled and used with a CCD sensing element to distinguish atomic spectra. Two versions of the microsystem have been implemented: planar and a capillary tube-based device. Detection of Cr and other chemicals in water samples has been successfully demonstrated with both devices.

I. INTRODUCTION

Biological and chemical threats to our drinking water exist from accidental and intentional pollutant sources. Water chemistry testing involves sampling the water supply on-site, and transporting the water sample to a laboratory. Inorganic pollutants are currently measured with a plasma spectrometer, a fairly large and elaborate machine. A field portable device would provide an instant and less expensive means of water testing, and would reduce possible cross contamination of transported samples. Our group has previously reported the LED-SpEC chip, a miniature discharge source for water contaminants detection [1]. Impurity concentration is found from the ratio of a signature emission strength to that of a reference, such as atmospheric nitrogen. The present effort involves the integration of a microspectrometer with the LED-SpEC chip, to build a more cost-effective, robust and portable water chemistry analysis microsystem. In contrast to the proof-of-concept device in [1], the dispersion optics in the new structure allows it to interface directly with a CCD camera without an external spectrometer. This is important because it allows the device to be arrayed in parallel for combinatorial analyses. In addition, the fluid handling and electrode configuration has been re-engineered for reliability and robustness.

There have been a number of sensor designs which use miniaturized spectrometers [2-5]. The unique feature of this microsystem is that an on-chip microdischarge source is utilized, so no other external laser or plasma source is required for sensor operation. This provides a more compact

microsystem. An additional new feature is that blazed gratings are used as the dispersion element to maximize the power in the diffraction order of interest, resulting in considerable improvement of the diffraction efficiency of the system, compared to previously reported binary amplitude grating based sensors. Our current system does not utilize collimation optics; we explore the possibility of using simplified optics, and evaluate the resulting compromises in resolution.

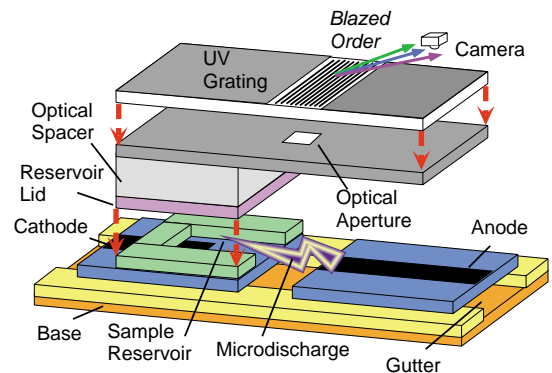


Fig. 1a: Exploded view of the “planar” device. The thick arrows indicate how the system is assembled

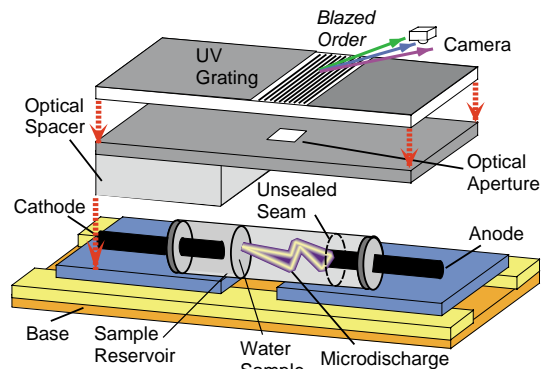


Fig. 1b: Schematic of the “capillary tube” device. The structure is held vertically during operation

II. MICROSYSTEM DESIGN

System Structure

Two versions of the system have been implemented, a “planar” and a “capillary tube” version. The planar version (Fig. 1a), is multi-layer glass device that includes a water sample reservoir, metal anode, optical aperture, and blazed grating. The assembly is held vertically during operation.

The capillary tube version (Fig. 1b), intended for low-cost, non-lithographic manufacturing, utilizes a glass capillary for the water reservoir and micro-discharge. Even though this version is usually held vertically during operation, it can also be held horizontally because the high capillary tension keeps the water sample in place.

The microdischarge source is similar in operation to the device previously reported [1]. An electric discharge is struck between a metal anode, and the water sample itself is used as the cathode. The water sample is energized through an immersed metal electrode. Ions from the microdischarge bombard the cathode water sample, and sputter the water and metal impurities into the discharge. The metal impurities then emit characteristic spectra, as does the nitrogen ambient. With respect to the device in [1], the fluid handling and electrode arrangements have been redesigned for improved reliability and robustness.

As opposed to standard transmission or reflection gratings, a *blazed* transmission grating is utilized for this design because of the following reasons: First, the transmission grating can be physically smaller, reducing the structural dimensions. Second, high-quality blazed gratings are commercially available in sizes appropriate for integration. Fabrication of planar (non-blazed) gratings require very tight metal linewidth tolerances, that may be incompatible with some processes. Lastly, blazed gratings offer superior diffraction efficiency, which dictates how much of the incident power is converted into useful signal. Maximum (100%) diffraction efficiency occurs when all optical power is delivered to one of the diffraction orders. Blazed gratings are theoretically capable of this, as the geometrical image transmitted through the grooves can be superimposed on a single diffraction order through proper choice of blaze angle [6]. The detector is a Sony DXC-107 CCD camera. It consists of 768×494 pixels, and each pixel is measured at $8 \mu\text{m} \times 9.5 \mu\text{m}$.

Modeling

A sketch of a transmission blazed grating is shown in Fig. 2. The direction of diffracted light is governed by the grating equation:

$$m\lambda = d(\sin\theta - \sin\theta_0) \quad (1)$$

where θ_0 is the incident angle, θ is the diffraction angle, λ and m are the wavelength and diffraction order and d is the spacing between adjacent grooves on the grating surface (Fig. 2). If the incident light is *collimated*, each groove of the grating forms an angle γ to the plane of the grating (Fig. 2). For a diffraction grating with N grooves, the diffraction intensity can be described as:

$$I = I_0 \left(\frac{\sin N\phi}{\sin\phi} \right)^2 \left(\frac{\sin\phi}{\phi} \right)^2 \quad (2)$$

$$\text{where } \phi = \frac{\pi}{\lambda} d(\sin\theta - \sin\theta_0),$$

$$\phi = \frac{\pi}{\lambda} d \cos\gamma \times (\sin(\theta - \gamma) - \sin(\theta_0 - \gamma)),$$

and 2ϕ is the phase difference between the center of the adjacent grooves (Fig. 2), ϕ is the phase difference between the center and edge of a single groove. The second term in eqn. (2) is also called the *blaze function*. and the relative intensity distribution for a specific incident wavelength can be obtained based on eqns. (1)-(2).

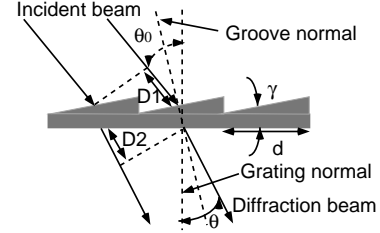


Fig. 2: Illustration of a transmission blazed grating.

An enlarged layout of the optical system, and operational components of the complete system is illustrated in Fig. 3a. The microdischarge, which is powered by an external source, is separated by a distance L_2 from the aperture using an optical spacer. Under this condition, the external CCD camera can capture the *blazed order* along with the geometric image (“zero” order) of the microdischarge. The blazed order is formed by constructive interference between a diffraction order, and the geometrical image transmitted by the angled grooves. This set-up allows the use of the “zero” and blazed order positions as a reference to calibrate the position of the dispersed wavelengths in the blazed order. A more compact optical scheme places the microdischarge in close proximity to the aperture (Fig. 3b). However, with this smaller design, the “zero” order cannot be captured by the CCD camera and only the blazed order is captured.

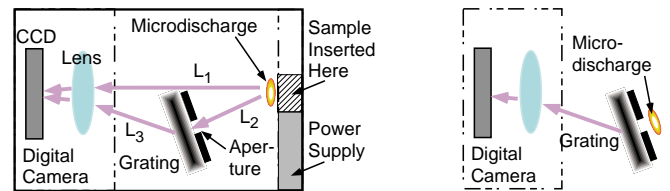


Fig. 3: (a-left): *Optical system A*, designed to include the geometric image of the microdischarge (not to scale). System only requires external camera and power supply for operation. (b-right): *Optical system B*, designed to exclude the geometric image.

MatLab™ simulations of both optical systems are shown in Fig. 4. The modeling parameters are as follows: The blazed grating has 600 grooves/mm, and a 22° blaze angle. The microdischarge source is assumed to be a Gaussian beam of width 0.3 mm. The average incident angle θ_0 (Fig. 2) is 5° . The spacing (L_3) between the camera and the grating is 35 cm as used in the experiments. The intensity of the Cr is 75% of that of the N_2 . The image size, through lens reduction of the camera, is 1/3 the real size of the microdischarge. The microdischarge is 13 cm (L_2) from

the grating for the optical arrangement in Fig. 3a and is 2.5 mm for Fig. 3(b). In addition, the microdischarge is assumed to be collimated. Figure 4 illustrates that N₂ (with a spectral line at 358 nm) and Cr (425 nm) can be readily distinguished.

The peak positions of the spectra of Cr and N₂ are modeled to have a 0.15 mm spacing, with a L₃ (Fig. 3) distance of 35 cm, and the calculated angular resolution ($\partial\theta/\partial\lambda$) is 0.22 rad/ μm for both optical systems. The angular dispersion is determined by the grating and the wavelengths of the incident light. Therefore, the spacing between the spectra of N₂ and Cr on the CCD camera for both optical arrangements shown in Fig. 3 should be the same, and only a function of L₃. As the CCD pixel spacing is 8 μm , L₃ of only 1.5 cm is required for spectral discrimination. In addition, for the optical system in Fig. 3a L₂ can be scaled down from 13 cm to < 8 mm, since the only requirement is to ensure the position of the microdischarge source is not blocked by the grating, thus can be imaged directly on the CCD sensor. In reality, the microdischarge is un-collimated, so the spectral peaks will be broader, while maintaining the same position.

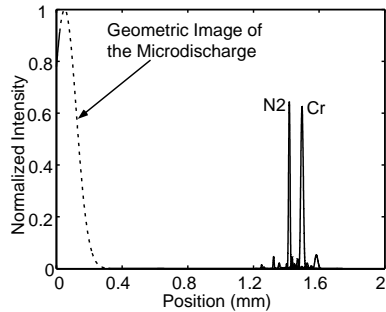


Fig. 4: Calculated spectrum from Cr contaminated water with the geometric image of the microdischarge (dashed line). Configuration in Fig. 3a excludes geometrical image.

III. EXPERIMENTAL RESULTS AND DISCUSSION

The optical micrographs of a sub-assembly and finished planar device are shown in Fig. 5. All layers are 506 μm thick, Pyrex™ #7740 glass except for the top layer, which is a blazed grating with 600 grooves/mm and a 22° blaze angle on 3 mm thick B270 Schott glass. The #7740 glass substrate is used because of its high transmittance, which is >80% at wavelengths ranging from 300 to 700 nm that are characteristic of metal impurities in water. For the water reservoir and discharge source, shown in Fig. 5a, each layer is processed separately before the stack is bonded together. This stack consists of 7 glass layers: the bottom two layers provide a substrate with a gutter that can drain excess water; the layer above them supports the electrodes, whereas the next two above this form the sidewalls and lid of the sample reservoir. The cathode is the water sample itself, while the anode is constructed from a 30 μm thick metal film for robustness. The top two layers, which are separated from the rest by a 2.5 mm thick spacer, form the optical dispersion element, including an aperture and diffraction grating (Fig. 5b).

The blazed grating was characterized with a 325 nm laser, and the results are shown in Fig. 6. Since the laser is highly collimated and monochromatic, the spots are purely diffraction-limited. The measured *angular separation* between the first two spots on the left is 0.198 radians, which corresponds to expected values. As expected, since the leftmost (blazed order) spot is the brightest, most diffraction power is delivered there.

Experiments have been performed using both optical systems described in Section II. Figure 7 shows measured results from the planar device, using the optical arrangement shown in Fig. 3a. The image from the camera is processed using the imaging toolbox in MatLab™ to obtain the relative intensity of the spectra. In contrast to the calibrating laser, the microdischarge source is a non-point, polychromatic, and un-collimated source, which distorts the spectral images. Despite this, the diffraction patterns created are clearly distinguishable. Figure 8 shows the spectra generated from the planar structure, with the optical scheme shown in Fig. 3b, in which the geometric image is excluded. Figure 9a shows a close-up view of the microdischarge between the anode and the water sample in a capillary tube. Figures 9b and 10 show spectra of samples tested in the capillary tube. Both results, for Cr and Na respectively, use the optical system in Fig. 3a. The measured positions and spacing of the spectra between Cr and N₂ (Figs. 7, 8, 9(b)) match the simulation predicted results.

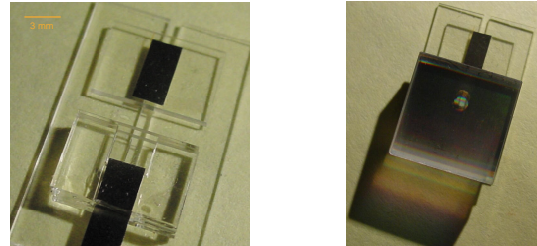


Fig. 5: Optical micrographs of a partially assembled (a-left) and finished planar device (b-right). Chip area is ~ 9 mm X 15 mm.

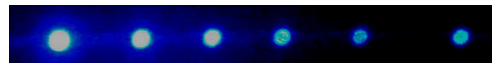


Fig. 6: Measured diffraction pattern from the blazed gratings using a 325 nm laser, showing blazed order on left.

For both optical systems shown in Fig. 3, without collimating optics, the spot size of the illumination source is one of the major factors influencing the resolution. It is found experimentally that the spot size of the microdischarge varies with the spacing between the anode and the cathode-water sample, and the shape of the sample reservoir. For example, comparing Fig. 7 to Fig. 9b, the spot size of the capillary design is more confined and smaller than that of the planar design under the same experimental conditions. The spectral peaks in Fig. 9b are narrower, especially for the N₂ signal. Therefore, minimizing spot size is important to improve the resolution of the system. However, optical

power is sacrificed by reducing the spot size. In order to maintain a reasonable signal to noise ratio (SNR), there is a tradeoff between the resolution and optical power.

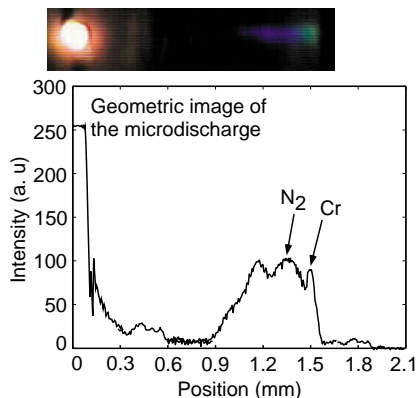


Fig. 7: Measured diffraction pattern obtained from a Cr contaminated water sample using the planar structure with optical sys. A.

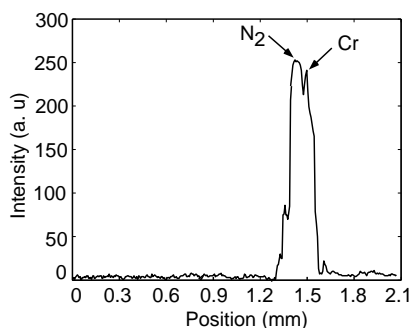


Fig. 8: Measured diffraction pattern from planar structure using Cr contaminated water sample (optical sys. B).

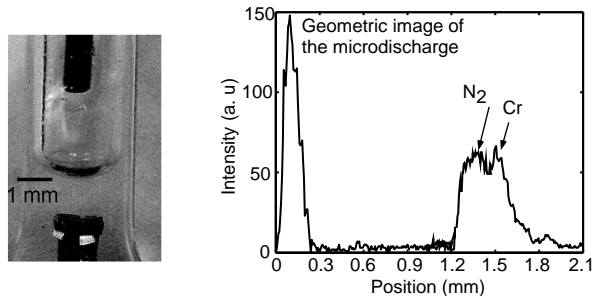


Fig. 9: (a-left): Close-up of capillary tube with diffraction grating removed, showing microdischarge; (b-right): Measured diffraction pattern obtained with capillary tube plasma using Cr contaminated water (optical sys. A).

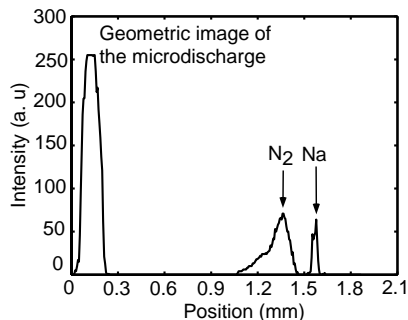


Fig. 10: Measured diffraction pattern obtained with capillary tube plasma using Na contaminated water.

The integration of collimating optics would improve both the spectral resolution, and would allow lower power operation. The broadening of spectral peaks is due to the non-point and un-collimated optical source. This could be mitigated by lenses, which would serve to collect more light, thereby allowing lower power operation of the microdischarge, or a greater signal level.

IV. CONCLUSIONS

Two device designs and two optical arrangements of an integrated microsystem for water chemistry analysis have been fabricated, and their performance evaluated. Attractive features of this system include an on-chip microdischarge as the optical source and an integrated blazed grating as the dispersion element. The first feature offers the opportunity to make the system more compact and cost effective; the second one improves the diffraction efficiency of the system greatly. In addition, the system can be easily arrayed in parallel for combinatorial analyses. Experiments show that the Cr and Na contaminants in the water and N₂ spectra can be detected without collimation optics. The spectral sensitivity is constrained by the 0.22 rad/μm radian angular resolution ($\partial\theta/\partial\lambda$) of the whole system. This resolution allows critical spectra to be distinguished without the use of collimation optics, and permits the separation between the grating and the camera to be reduced to 1.5 cm for 8 μm pixel spacing on the image plane.

ACKNOWLEDGEMENTS

The authors thank Mr. K. Udeshi for help with sample preparation, Dr. G. Zhao at University of Michigan for help with the grating characterization, and Drs. M. Anderson, W. Zeltner at University of Wisconsin-Madison and Prof. M. Zorn at University of Wisconsin-Green Bay for discussion on water chemistry. We would like to thank ISSYS, Inc. for use of their glass saw. This effort is supported in part by the National Science Foundation, the U.S. Geological Survey, and the Sea Grant.

REFERENCES

- [1] C.G. Wilson, Y.B. Gianchandani, "Spectral Detection of Metal Contaminants in Water Using an On-chip Microglow Discharge," *IEEE Trans. on Electron Devices*, (49)12 pp. 2317-22, 2002
- [2] G.M. Yee, N. Maluf, P.A. Hing, M. Albin and G.T.A. Kovacs, "Miniature spectrometers for biochemical analysis," *Sensors and Actuators*, A 58, pp. 61-66, 1997
- [3] D. Goldman, P. White and N. Anheier, "Miniaturized spectrometer employing planar waveguides and grating couplers for chemical analysis," *Appl. Optics*, 29, pp. 4583-4589, 1990
- [4] R. Riesenberger, G. Nitzsche, A. Wutting, B. Harnish, "Micro spectrometer and MEMS for space," 6th ISU Annual International Symposium, "Small Satellite: Bigger Business?" 21-23, May, 2001, Strasbourg, France
- [5] S.H. Kong, D.L. Wijngaards, R.F. Wolfenbittel, "Infrared micro-spectrometer based on a diffraction grating," *Sensors and Actuators*, A 92, pp. 88-95, 2001
- [6] M. Born and E. Wolf, "Principles of Optics", 7th Edition, Cambridge University, 1999